Dakota Graham
Mentor/Chair: Dr. Bradley Greger
Applied Project Final Report
4/29/2019

Changes in Neural Activity during Deep Brain Stimulation in Patients with Parkinson's Disease: Correlation with Stimulation Parameters, Tremor, and Outcomes

Abstract:

Deep brain stimulation (DBS) has been proven to be a safe and effective treatment for various neurological motor disorders such as Dystonia, Essential Tremor, and Parkinson's disease (PD). Since 1997, over 150,000 patients have undergone DBS implantation. DBS provides substantial clinical benefit to patients with PD, however, very little is known about the mechanisms by which DBS produces such a benefit. The goal of this project is to elucidate how DBS is interacting with neural physiology and provide insight into the mechanisms by which symptoms are ameliorated in PD. Understanding of DBS mechanisms would help drive development of more specialized DBS systems and open avenues for use in other pathologies. We recorded neural signals from patients with PD at the Barrow Neurological Institute (BNI) during the implantation of DBS leads while under general anesthesia. Neural signals were recorded using a microelectrode placed in the subthalamic nucleus (STN) during stimulation with the DBS lead. Stimulation frequency was varied during the recording as this is a key tuning parameter for device programming. We examined changes in action potential (AP) firing rates and the AP aligned average local field potentials (LFP) at various stimulation frequencies. There was an increase in RMS of AP aligned average LFP during stimulation at each of the stimulation frequencies. However, the largest increase was observed during stimulation within the typical therapeutic frequency range(140Hz). We speculate that DBS stimulation may be restoring a more natural relationship between APs and LFPs in the Basal Ganglia. Future work will include stimulation and recording while the patient is awake and incorporation of a tremor measurement system. This will reduce possible anesthesia confounds and allow us to directly link DBS stimulation frequency and tremor reduction to the observed changes in neural activity.

1. Introduction

Deep brain stimulation (DBS) has been proven to be a safe and effective treatment for various neurological motor disorders such as Dystonia, Essential Tremor, and Parkinson's disease (PD). Other neurological disorders are also treated but with less frequency. Since DBS was FDA approved for PD in 1997 over 150,000 DBS devices have been implanted [21]. Despite a relatively long history of efficacy, the mechanisms by which DBS provides benefit remain elusive. Many theories have been proposed for the mechanisms of DBS. These typically call back to an early theory that DBS acts as a reversible lesion. For instance, Welter et al. [11] showed that cell firing rate decreased during stimulation greater than 40Hz. Multiple studies have also shown not only a change in firing rate, but a change in firing pattern [32]. One hypothesis derived from a regularization in firing pattern is a so called "informational lesion" in which a reduction in entropy results in a decrease of information transfer [5]. Contrary to this theory is another that states regularization in cell firing compensates for a lack of information processing capabilities of the thalamocortical system [32], [16]. Although many theories exist, there still remains much uncertainty about mechanisms of DBS. This being said, patients are able to achieve remarkable benefit. Through trial and error many studies have identified therapeutic ranges of DBS parameters. The therapeutic frequency range for subthalamic nucleus DBS (for PD) is 135-185Hz [8]. Patients typically receive the most benefit within this range little to no benefit outside the range. It was also discovered that low frequency stimulation (<10Hz) actually results in a worsening of motor control for PD patients [12]. This paper will focus primarily on identifying changes in neural activity during DBS at different frequencies in patients with Parkinson's disease.

Parkinson's disease (PD) is a neurological disorder affecting an estimated 10 million people worldwide [2]. Symptoms include tremor, bradykinesia (slowed movement), rigidity, impaired posture and balance, and speech changes [23]. Several factors play a role in the cause of Parkinson's disease, such as hereditary genetic mutations and environmental triggers (exposure to toxins). Parkinson's disease has been linked to a decrease in dopamine levels caused by neurodegeneration in the substantia nigra (cells that produce dopamine). It has recently been shown that synaptic dysfunction may be causing the neurodegeneration as opposed to actual cell death [31]. This is thought to be caused by aggregation of α-synuclein at the synapses of cells, preventing cell firing. PD symptoms are initially managed through pharmaceutical intervention, however, as the disease progresses medication becomes ineffective or patients experience intolerable side-effects. These are heavily weighted metrics in determining candidacy for DBS.

The DBS procedure involves implanting leads into the basal ganglia as well as an internal pulse generator (IPG) subcutaneously in the patient's chest to power the electrodes. For Parkinson's disease, the target is either the Subthalamic Nucleus (STN) or Globus Pallidus interna (GPi) depending on symptom presentation. The benefits of choosing STN are a greater reduction in medications and fewer battery changes [29]. Benefits of targeting the GPi include better control of dyskinesias, easier programming, and more flexible medication management [29]. After the DBS system is implanted, a neurologist programs the device for optimal tremor reduction by manipulating voltage amplitude (or current amplitude), frequency, and pulse width. DBS leads are implanted while the patient is lightly sedated "awake" or under general anesthesia "asleep". The latter just recently being proven to be as safe and effective as the former which was the previous labeling by the FDA. Recordings in this study were gathered while the patient

was “asleep” by placing a microelectrode in the STN. During recording, the DBS lead was used to stimulate at various frequencies spanning the capabilities of the device.

The goal of this project is to gain a better understanding of the relationship between deep brain stimulation and physiological changes that result in tremor reduction. This may help drive development of more specialized DBS systems and open avenues for the use of DBS in other pathologies. This will be achieved through several specific aims:

Specific Aims

Specific aim 1: Obtain intraoperative microelectrode recording from single neurons in the STN.
Specific aim 2: Analyze effect of DBS on action potentials and local field potentials.
Specific aim 3: Correlate changes in APs and LFPs with reductions in tremor.

2. Methods

2.1 Microelectrode Recording

Recordings were performed on four patients with Parkinson’s disease at one site, the Barrow Neurological Institute (BNI). The patients were sedated using general anesthesia. A minimal amount of anesthesia was used to reduce suppression of neural activity. Recordings were gathered using a platinum-iridium microelectrode placed in the STN during stimulation. A standard image guidance platform was used to target the STN for both the DBS electrode and the microelectrode. The microelectrode was placed either on the same side as the stimulating electrode (ipsilateral) or opposite side (contralateral). Only one electrode was chosen to stimulate from during the recording.

Stimulation was performed using the Medtronic 3387 DBS lead and connected to the standard programmer used for intraoperative stimulation testing. Constant voltage stimulation was used and held at 3V. Frequencies of stimulation were manually changed between blocks (groups of stimulation trials and corresponding baseline) and the stimulation manually turned on and off for each trial. These frequencies include 20, 70, 140, and 250Hz. Stimulation blocks were performed out of ascending order (140, 20, 250, and 70) to remove effects of a linear increase in stimulation.

The recording/stimulating procedure can be visualized in Figure (1). Before stimulation is turned on, a baseline recording is performed. Stimulation is then turned on for ten seconds, then off for ten seconds, and repeated ten times. This will be referred to a ‘block’. A total of four blocks were performed for each patient, corresponding to the four stimulation frequencies: 20, 70, 140, and 250Hz.

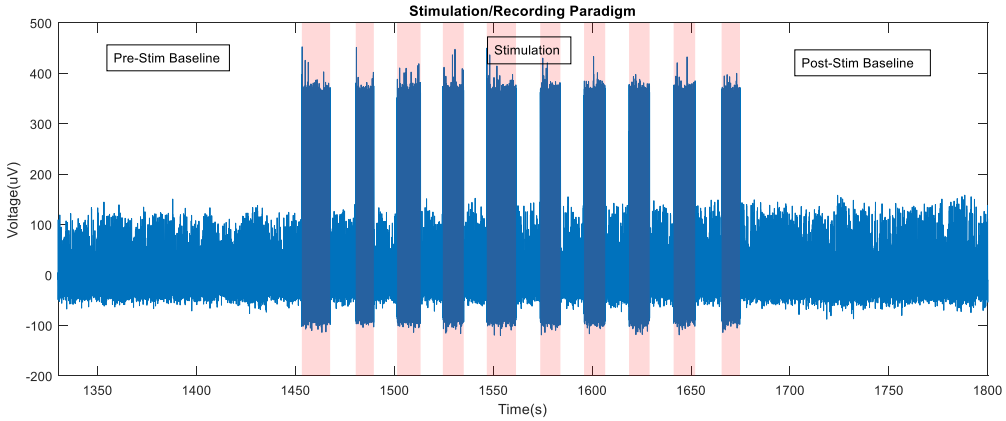

Figure 1: Single recording block including a baseline recording prior to stimulation. Stimulation shown in pink. And a baseline recording for the upcoming block after stimulation.

The second ipsilateral patient recorded from will be excluded from analysis due to substantial low frequency noise. This noise is present through most all of the recording and obliterates structure of the local field potential. During a period of low noise, LFP amplitude stays below 500uV. While noise is present the LFP nearly reaches 2000uV. A comparison of these two signals can be seen in Figure (A1) in the appendix.

2.2 Action Potential Analysis

After filtering was performed, a three-parameter thresholding technique was used to identify action potentials and stimulation artifacts. These parameters include minimum amplitude, minimum spike width, and maximum spike width. Figure (2) shows the high-pass filtered data for visualizing the difference between stimulation artifacts and action potentials. This figure shows contralateral recordings. Stimulation artifacts during ipsilateral recordings are significantly larger (several thousand microvolts) since the recording electrode is much closer to the stimulating electrode. The stimulation artifacts were subtracted out of the signal leaving only the action potentials which were then sorted using principal component analysis (PCA).

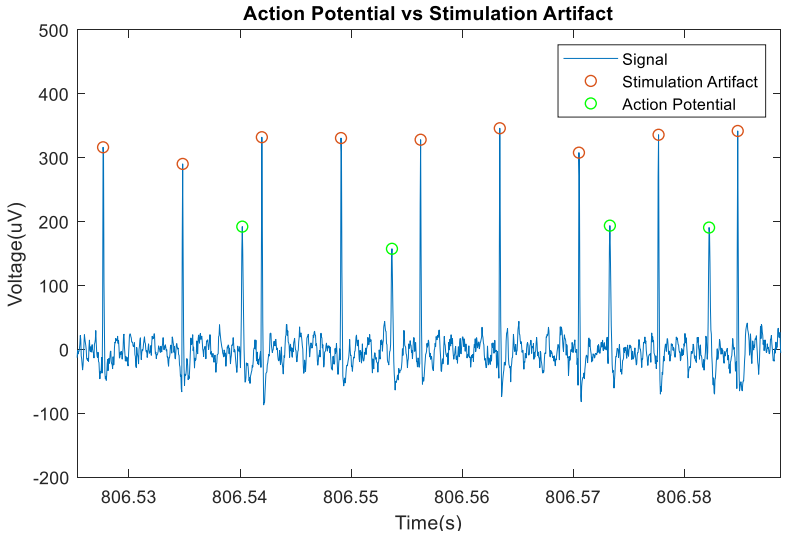

Figure 2: Contralateral Patient #1. Distinguishing stimulation artifacts from action potentials. Orange circles mark the stimulation artifacts and green mark the action potentials.

The maximum number of clusters used for conducing PCA was first set to five to capture all possible neurons within reason. Next, both the waveshape and PCA cluster plots were visualized to identify which neurons should be grouped together/separately. Through trial and error, the ideal number of clusters was chosen. Visualization of firing rate for the different units was also checked to help with identifying neurons that should have been grouped together. Figure (3) illustrates a comparison of the average action potential waveshape of two neurons clustered using PCA. These were deemed to be different neurons based primarily on amplitude.

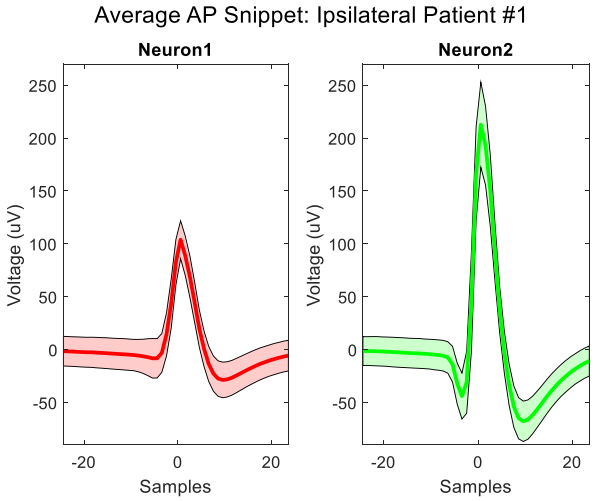

Figure (3): Average action potential waveform and standard deviation of two neurons isolated using PCA.

Once individual neurons were identified based on wave shape and amplitude, a spike-train of each cell was constructed, and a binning technique was used to determine variations in firing rate that was then mapped onto the periods of stimulation. A plot of firing rate for each neuron can be seen in Figure (4). When analyzing the firing rate of the cell, the amount of neural activity lost due to removal of stimulation artifact need to be considered. It was concluded that the two neurons isolated and shown in Figure (3) were indeed unique.

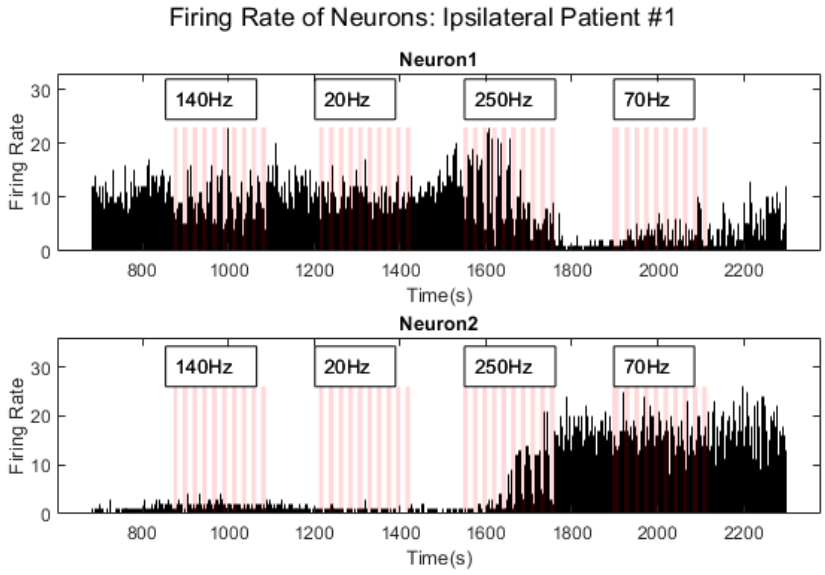

Figure (4): Firing rate histograms of two neurons isolated using PCA.

2.3 Verifying Recording/Macro-analysis

While recording, a real-time plot of high-pass filtered signal was visualized to aid in locating an active neuron and to verify that the action potential firing pattern matches with what is expected in the STN. An image obtained from Starr et al. [34] displaying the various cell firing patterns in nuclei near the STN can be seen in the appendix, Figure (A2). Patients who underwent DBS implantation revealed similar findings as reported by Steigerwald et al. [20] with a characteristic "bursty" firing pattern. This can be seen in Figure (5), which is a plot of baseline recording.

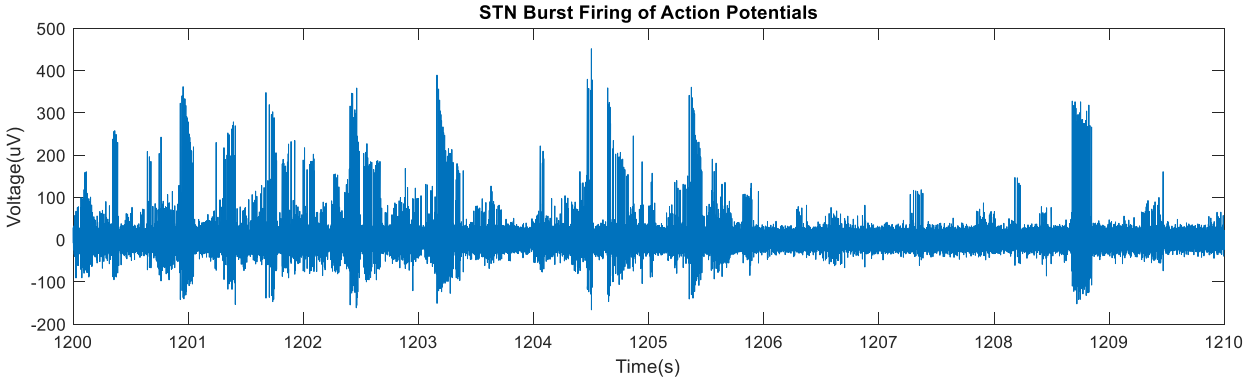

Figure (5): Baseline recording of cells in STN. Burst firing of cells is observed.

Although these cells match the typically seen burst firing pattern, it may be of importance to note that these cell firing patters are more complex than those discussed in literature that was reviewed. During a single burst, the cell firing rate will increase from about 125Hz (at beginning of burst) to 330Hz by the end of the burst. The action potential amplitude will also decrease from about 400uV to 200uV by the end of the burst. An image of this can be seen in Figure (6). This particular burst was obtained from the same data used in the previous figure, now zoomed in on a 300ms segment.

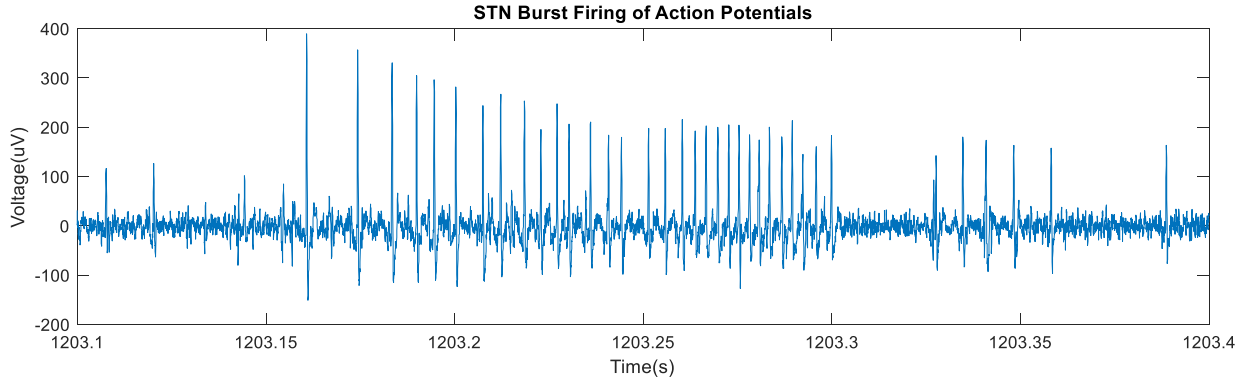

Figure (6): Zooming in on a single burst of action potentials allows for visualizing of more complex firing pattern. This includes a decrease in amplitude (400uV to 200uV) and an increase in firing rate (from 125Hz to 330Hz).

These changes in frequency and amplitude are may be another layer of encoding information that has not been thoroughly explored. Analysis of the complex burst firing is not within the scope of this paper, but it was important to take into consideration when performing spike-sorting to ensure cells were grouped appropriately.

2.4 AP Aligned LFP Analysis

Action potential aligned average local field potentials (APAALFPs) were calculated to investigate the phase relationship between action potential firing and local field potentials in the STN. This involved obtaining the LFP about an action potential (before and after) as can be seen in Figure (7). For this particular example a window of 600ms was used to capture 300ms of LFP before and 300ms after an action potential was observed. However, in the data to be presented a 500ms window was used. A bandpass filter from 3-55Hz was used isolate broadband local field potentials while avoiding power line noise (60Hz). For this analysis, all potential neurons were grouped together to obtain multiunit APAALFP.

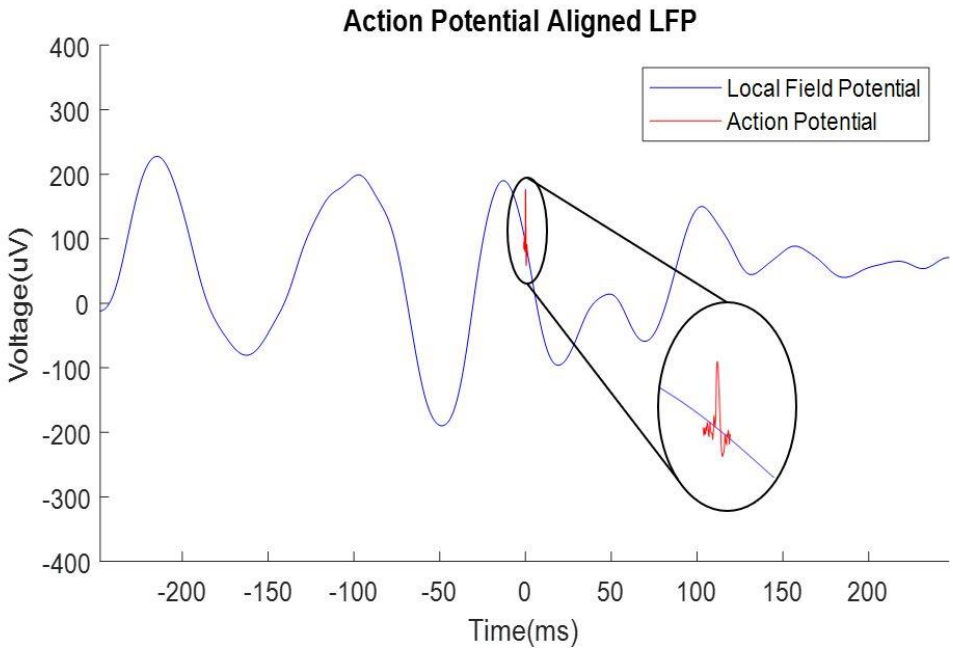

Figure (7): Illustration of action potential aligned LFP. The red waveform represents an action potential and the blue waveform represents the LFP associated with that action potential.

2.5 Statistical Analysis of AP Aligned LFP

Due to variations in cell firing and length of recordings between groups (Stim ON, Stim OFF, and Baseline), the amount of action potentials captured for each group varied greatly. This was a concern because the RMS of the APAALFPs appeared to be dependent on the AP count. A comparison of RMS and AP count can be seen in Figure (8).

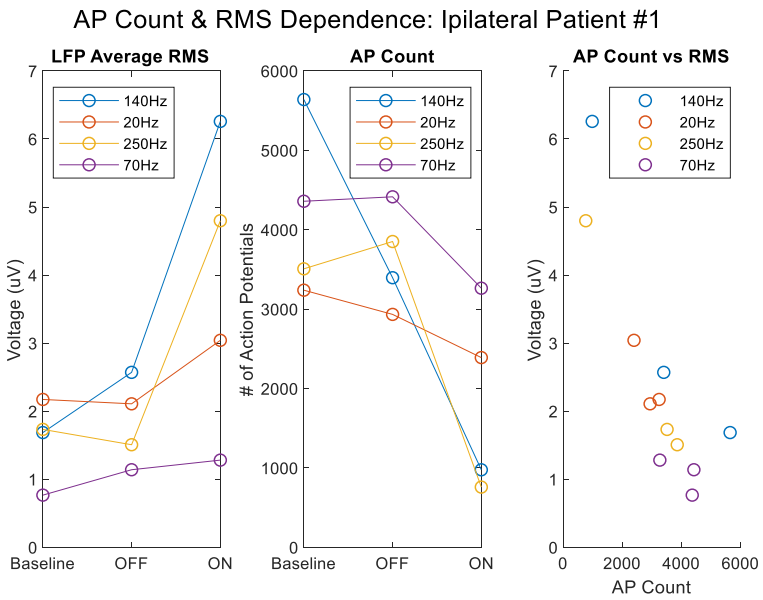

Figure (8): Illustrates the relationship between APAALFP RMS and the AP count. Each group is represented by a different color. The left most graph shows the APAALFP RMS for each group, the middle shows the AP count, and the right shows them plotted against each other.

As seen in Figure (8), an increasing trend in LFP RMS and a corresponding deceasing trend in AP count suggests dependency. Steps were taken to ensure that the changes in APAALFP RMS were not purely a response to changes in AP count. Bootstrapping was used to randomly sample the groups with a fixed AP count, thereby removing confounds of AP count on APAALFP. An AP count of approximately 93% of the smallest observed was used. An AP count of 700 was used for all patients. Each group was randomly sampled 1000 times (Epochs) to ensure the sample space was adequately explored. The average RMS values after utilizing bootstrapping can be seen in Figure (9). It should be noted that the standard deviation (SD) during 250Hz stimulation is much lower than the SD of other groups. This is because the chosen AP count of 700 is closets to the total AP count of that group (758). The next closest is stimulation ON at 140Hz with a total AP count of 972.

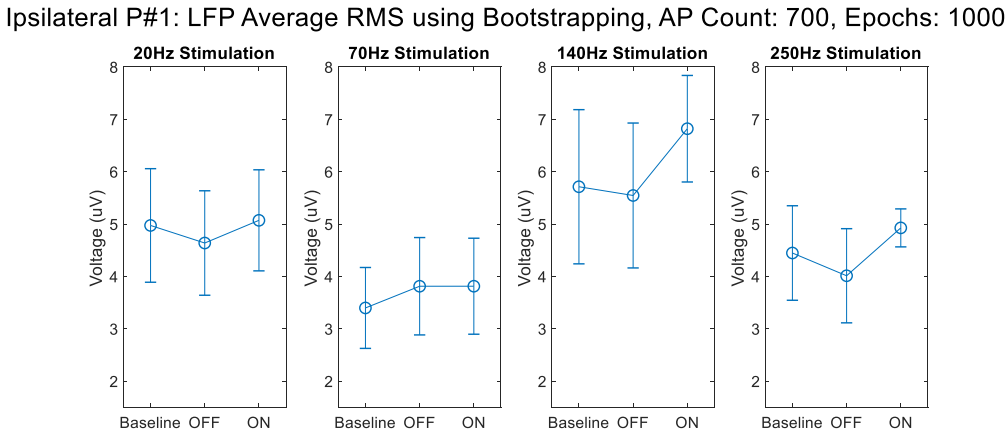

Figure (9): Average RMS of APAALFP after bootstrapping with standard deviation error bars.

To better visualize the changes in APAALFP, the RMS values of ON and OFF stimulation were normalized to the baseline recorded prior to stimulation. The percent change from mean baseline RMS was then calculated and plotted as a bar chart. A one-way ANOVA was performed to determine significance of these percent changes from baseline. One condition of an ANOVA is that data come from a normally distributed population. Histograms of all groups were calculated to determine appropriateness of an ANOVA. These can be seen for the first ipsilateral patient in Figure (10). Although some samples appear to have a slight skew, the data was deemed close enough to a normal distribution for use of an ANOVA.

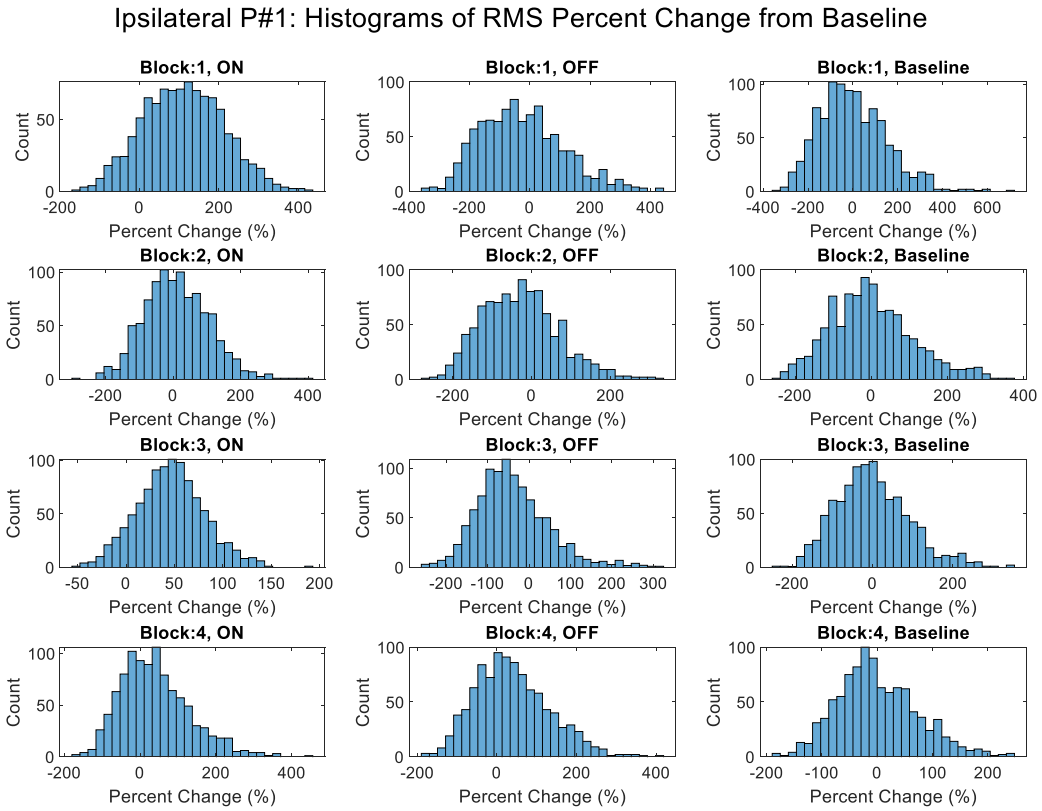

Figure (10): Histogram of each group to check for normal distribution. No obvious skewed distributions observed.

3. Results

3.1 Action Potential Aligned Average LFP

Action potential aligned LFP averaged across all APs within each group for Ipsilateral Patient #1 can be seen in Figure (11). An increase in amplitude of APAALFP during stimulation at high frequencies was observed. In contrast, recordings from the contralateral side did not exhibit an increase in amplitude of APAALFP during stimulation. Recordings from contralateral patients can be seen in the appendix, Figure (A3) and Figure (A4) respectively. As mentioned previously, these results are confounded by the large variations in AP count per group. To account for this, bootstrapping was used to analyze changes in APAALFP RMS.

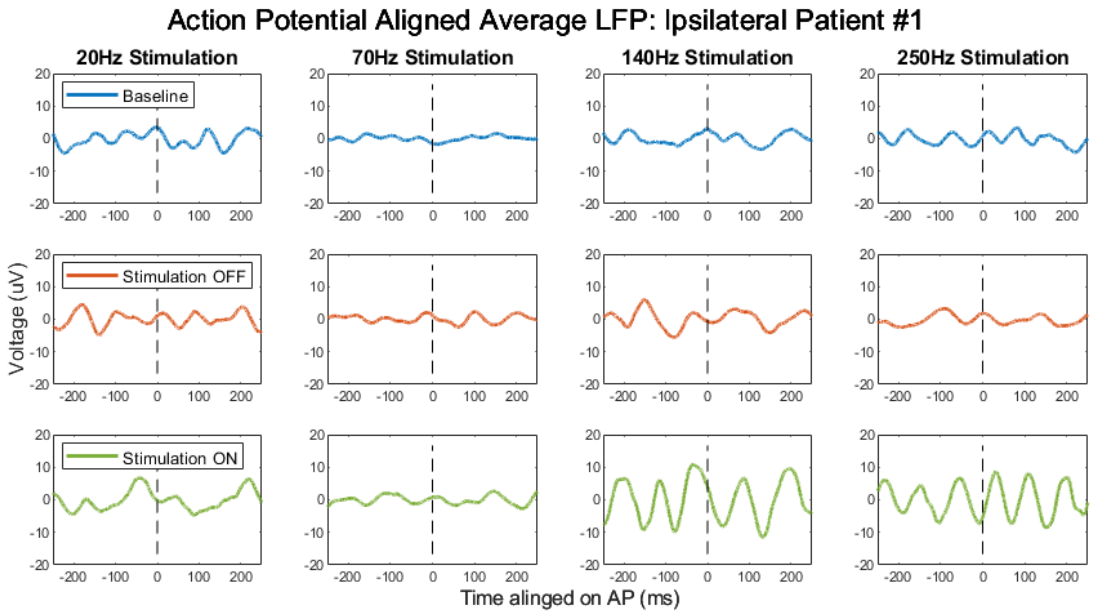

Figure (11): Plot of action potential aligned average LFPs for each group. Blue signals indicate baseline recordings, red indicate stimulation OFF, and green indicate stimulation ON. This shows an increased amplitude of low frequency oscillations for the stimulation ON groups of 140 & 250Hz stimulation.

Results of bootstrapping for the 1st Ipsilateral Patient can be seen in Figure (12). The RMS of LFP increased 110% during 140 Hz stimulation compared to baseline. Stimulation at 70 Hz and 250 Hz yielded increase of 41% and 48% respectively. Low frequency stimulation at 20 Hz yielded a 10% increase from baseline. Conducting a multiple comparisons test with an alpha value of 0.001 yielded statistical significance between all groups except on and off stimulation at 70Hz.

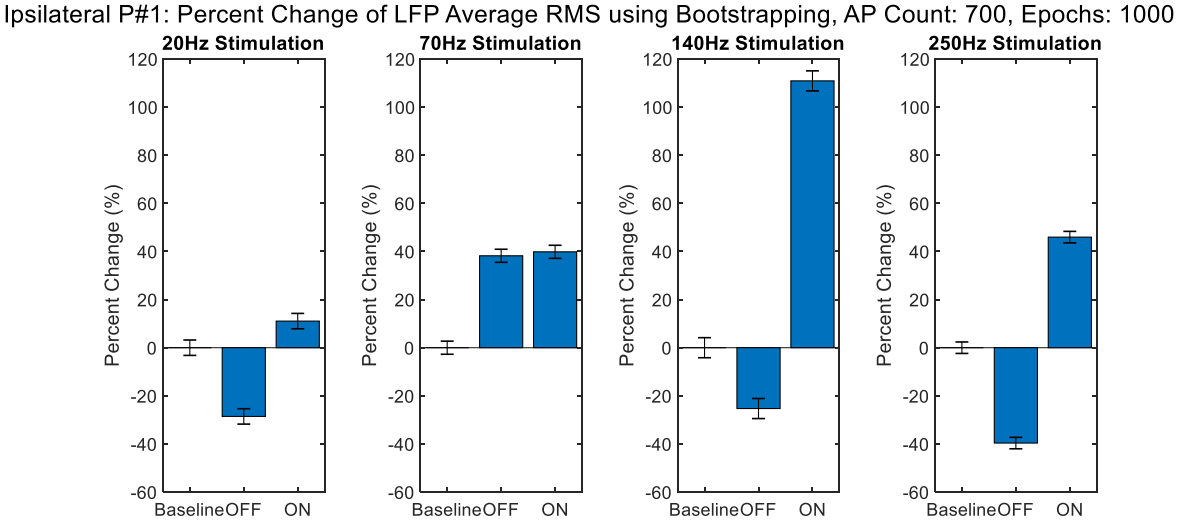

Figure (12): Ipsilateral Patient #1. Percent change of APAALFP RMS from baseline. Error bars represent standard error. All values are statistically significant except for ON/OFF of 70Hz stimulation.

Percent changes in APAALFP for the Contralateral Patients 1&2 can be seen in the appendix, Figure (A5) and Figure (A6) respectively. Although no patterns are seen between contralateral patients, it is clear that the percent changes from baseline during high frequency stimulation are significantly smaller than that those seen in the ipsilateral side. In some cases, the RMS during stimulation is lower than baseline.

4. Discussion

Patients with PD typically receive bilateral DBS lead placement. This is because stimulation of a single STN will only result in tremor reduction for the corresponding limb(s). We would expect to see greater modulation of neural activity in the STN where the DBS electrode is placed since this will correspond to limb receiving tremor reduction. In contrast we would expect to see no change in neural activity on the contralateral STN. Results showed large increases in LFP RMS during stimulation at high frequencies on the same side (ipsilateral), as well as little to no increase in LFP RMS during stimulation on the opposite side (contralateral).

The therapeutic range of DBS for PD is 135-185Hz [8]. We expect to see the largest modulations of LFP during stimulation within this frequency range. APAALFP RMS exhibited the largest increase from baseline during stimulation at 140Hz, while stimulation at 70 & 250Hz yielded approximately half the percent increase from baseline. If LFP RMS amplitude was simply proportional to stimulation frequency, we would expect stimulation at 250Hz to yield a larger LFP increase than 140Hz. This shows that LFP RMS is not merely increasing due to an increase in stimulation frequency but is correlated with clinically effective stimulation frequencies. The smallest change in RMS was seen during 20Hz stimulation, which is the stimulation frequency furthest from the therapeutic range. These results suggest that an increase in APAALFP RMS may correlate with a decrease in tremor and an improvement in motor control. Based on this finding, we speculate that DBS is restoring a more ideal phase relationship between APs and LFP. However, these speculations are assuming the unanesthetized Basal Ganglia circuitry will respond similarly to DBS and that the chosen stimulation parameters would invoke benefit in the awake patient.

5. Conclusion & Future Work

In summary, our results reflect a correlation between action potential aligned LFP RMS and the typical therapeutic range seen in DBS. However, without directly measuring tremor reduction during stimulation, these conclusions remain highly speculative and dependent on the assumption that the patient would have received clinical benefit at the stimulation frequencies performed. Future work will include a more thorough analysis of the frequency domain and performing these experiments while the patients are only lightly sedated so that tremor can be observed. Tremor will be monitored using an accelerometer attached to the patient's wrist. The hardware setup can be seen in the appendix, Figure (A10). This will allow us to directly link changes in neural activity with changes in tremor.

References:

[1] J. Gardner, “A history of deep brain stimulation: Technological innovation and the role of clinical assessment tools,” Soc Stud Sci, vol. 43, no. 5, pp. 707–728, Oct. 2013.
[2] R. Swain-Eng, “American Academy of Neurology,” p. 56.
[3] H. Bokil, P. Andrews, J. E. Kulkarni, S. Mehta, and P. Mitra, “Chronux: A Platform for Analyzing Neural Signals,” J Neurosci Methods, vol. 192, no. 1, pp. 146–151, Sep. 2010.
[4] A. Wagle Shukla, P. Zeilman, H. Fernandez, J. A. Bajwa, and R. Mehanna, “DBS Programming: An Evolving Approach for Patients with Parkinson’s Disease,” Parkinson’s Disease, 2017. [Online]. Available: https://www.hindawi.com/journals/pd/2017/8492619/. [Accessed: 08-Apr-2019].
[5] W. M. Grill, A. N. Snyder, and S. Miocinovic, “Deep brain stimulation creates an informational lesion of the stimulated nucleus,” Neuroreport, vol. 15, no. 7, pp. 1137–1140, May 2004.
[6] “Deep brain stimulation of the internal capsule enhances human cognitive control and prefrontal cortex function | Nature Communications.” [Online]. Available: https://www.nature.com/articles/s41467-019-09557-4. [Accessed: 20-Apr-2019].
[7] “Deep-Brain-Stimulation-Guide-Parkinsons.pdf.” .
[8] R. Ramasubbu, S. Lang, and Z. H. T. Kiss, “Dosing of Electrical Parameters in Deep Brain Stimulation (DBS) for Intractable Depression: A Review of Clinical Studies,” Front Psychiatry, vol. 9, Jul. 2018.
[9] gfa, “Eavesdropping on Neurons,” Harvard University Brain Tour. .
[10] E. B. Montgomery, “Effects of GPi stimulation on human thalamic neuronal activity,” Clinical Neurophysiology, vol. 117, no. 12, pp. 2691–2702, Dec. 2006.
[11] M.-L. Welter et al., “Effects of High-Frequency Stimulation on Subthalamic Neuronal Activity in Parkinsonian Patients,” Arch Neurol, vol. 61, no. 1, pp. 89–96, Jan. 2004.
[12] A. Eusebio et al., “Effects of low-frequency stimulation of the subthalamic nucleus on movement in Parkinson’s disease,” Exp Neurol, vol. 209, no. 1, pp. 125–130, Jan. 2008.
[13] A. Shah et al., “Intraoperative acceleration measurements to quantify improvement in tremor during deep brain stimulation surgery.,” Medical & biological engineering & computing, vol. 55, no. 5, pp. 845–858, 2017.
[14] C. Seifried et al., “Intraoperative microelectrode recording for the delineation of subthalamic nucleus topography in Parkinson’s disease,” Brain Stimulation, vol. 5, no. 3, pp. 378–387, Jul. 2012.
[15] T. M. Herrington, J. J. Cheng, and E. N. Eskandar, “Mechanisms of deep brain stimulation,” J Neurophysiol, vol. 115, no. 1, pp. 19–38, Jan. 2016.
[16] E. B. Montgomery and K. B. Baker, “Mechanisms of deep brain stimulation and future technical developments,” Neurol. Res., vol. 22, no. 3, pp. 259–266, Apr. 2000.
[17] C. R. Camalier et al., “Methods for Surgical Targeting of the STN in Early-Stage Parkinson’s Disease,” Front. Neurol., vol. 5, 2014.
[18] “Micro-Electrode Recording | Neurosurgery | University of Pittsburgh.” [Online]. Available: http://www.neurosurgery.pitt.edu/centers-excellence/clinical-neurophysiology/micro-electrode-recording. [Accessed: 30-Jan-2019].
[19] T. Heida and J. Modolo, “Models of deep brain stimulation,” Scholarpedia, vol. 12, no. 8, p. 33311, Aug. 2017.
[20] F. Steigerwald et al., “Neuronal Activity of the Human Subthalamic Nucleus in the Parkinsonian and Nonparkinsonian State,” Journal of Neurophysiology, vol. 100, no. 5, pp. 2515–2524, Nov. 2008.
[21] “Newsroom | Medtronic | RSS Content.” [Online]. Available: http://newsroom.medtronic.com/phoenix.zhtml?c=251324&p=RssLanding&cat=news&id=2279215. [Accessed: 27-Mar-2019].

[22] “Parkinson’s disease - Diagnosis and treatment - Mayo Clinic.” [Online]. Available: https://www.mayoclinic.org/diseases-conditions/parkinsons-disease/diagnosis-treatment/drc-20376062. [Accessed: 29-Jan-2019].
[23] “Parkinson’s disease - Symptoms and causes,” Mayo Clinic. [Online]. Available: https://www.mayoclinic.org/diseases-conditions/parkinsons-disease/symptoms-causes/syc-20376055. [Accessed: 29-Jan-2019].
[24] M. A. Andersen et al., “Parkinson’s disease-like burst firing activity in subthalamic nucleus induced by AAV-α-synuclein is normalized by LRRK2 modulation,” Neurobiology of Disease, vol. 116, pp. 13–27, Aug. 2018.
[25] J. R. Walters, D. Hu, C. A. Itoga, L. C. Parr-Brownlie, and D. A. Bergstrom, “Phase relationships support a role for coordinated activity in the indirect pathway in organizing slow oscillations in basal ganglia output after loss of dopamine,” Neuroscience, vol. 144, no. 2, pp. 762–776, Jan. 2007.
[26] “Statistics on Parkinson’s Disease | Parkinson Association of the Carolinas.” [Online]. Available: https://www.parkinsonassociation.org/facts-about-parkinsons-disease/. [Accessed: 31-Jan-2019].
[27] M. Filali, W. D. Hutchison, V. N. Palter, A. M. Lozano, and J. O. Dostrovsky, “Stimulation-induced inhibition of neuronal firing in human subthalamic nucleus,” Exp Brain Res, vol. 156, no. 3, pp. 274–281, Jun. 2004.
[28] D. Charles et al., “Subthalamic nucleus deep brain stimulation in early stage Parkinson’s disease,” Parkinsonism & Related Disorders, vol. 20, no. 7, pp. 731–737, Jul. 2014.
[29] N. R. Williams, K. D. Foote, and M. S. Okun, “Subthalamic Nucleus Versus Globus Pallidus Internus Deep Brain Stimulation: Translating the Rematch Into Clinical Practice,” Mov Disord Clin Pract, vol. 1, no. 1, pp. 24–35, Apr. 2014.
[30] A. A. Kühn, T. Trottenberg, A. Kivi, A. Kupsch, G.-H. Schneider, and P. Brown, “The relationship between local field potential and neuronal discharge in the subthalamic nucleus of patients with Parkinson’s disease,” Experimental Neurology, vol. 194, no. 1, pp. 212–220, Jul. 2005.
[31] W. J. Schulz-Schaeffer, “The synaptic pathology of α-synuclein aggregation in dementia with Lewy bodies, Parkinson’s disease and Parkinson’s disease dementia,” Acta Neuropathol, vol. 120, no. 2, pp. 131–143, Aug. 2010.
[32] S. Santaniello, M. M. McCarthy, E. B. Montgomery, J. T. Gale, N. Kopell, and S. V. Sarma, “Therapeutic mechanisms of high-frequency stimulation in Parkinson’s disease and neural restoration via loop-based reinforcement,” PNAS, vol. 112, no. 6, pp. E586–E595, Feb. 2015.
[33] B. I. Reports, “World Deep Brain Stimulation Market Double Digit Growth Rate Forecasts To 2025,” Medium, 11-Dec-2017.
[34] P. A. Starr et al., “Implantation of deep brain stimulators into the subthalamic nucleus: technical approach and magnetic resonance imaging-verified lead locations.,” Journal of neurosurgery, vol. 97, no. 2, pp. 370–387, 2002.

Appendix:

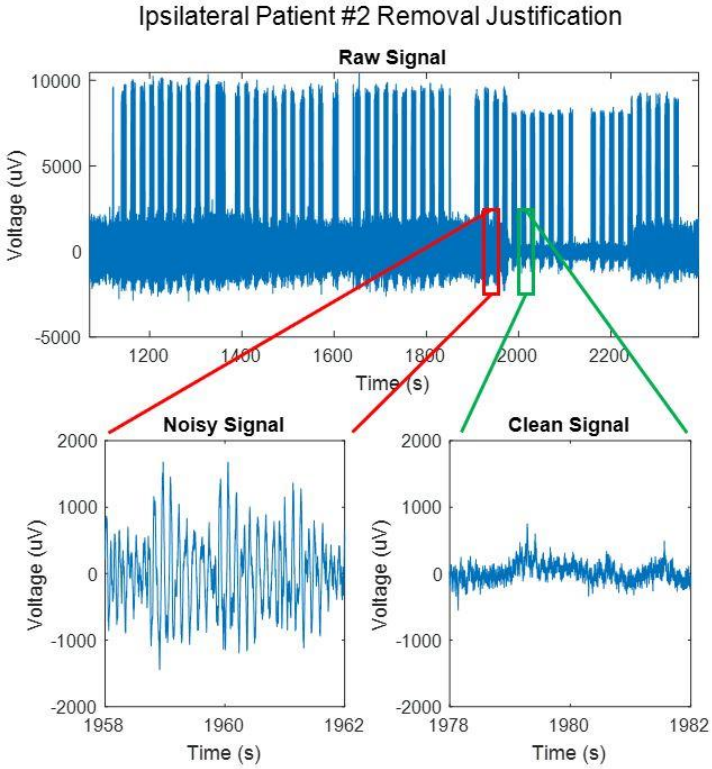

Figure (A1): Raw signal of ipsilateral patient #2 is shown in the top plot. Subsequent plots show four second snippets of noisy and clean signal. Large amplitude, low frequency noise dominates much of the recoding.

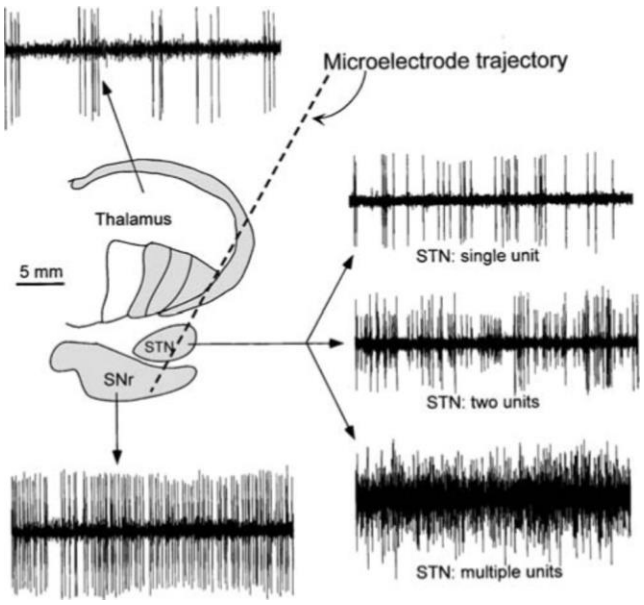

Figure (A2): This image was created by Starr et al. [34] and depicts the various cell firing patterns along the implantation tract of a DBS electrode.

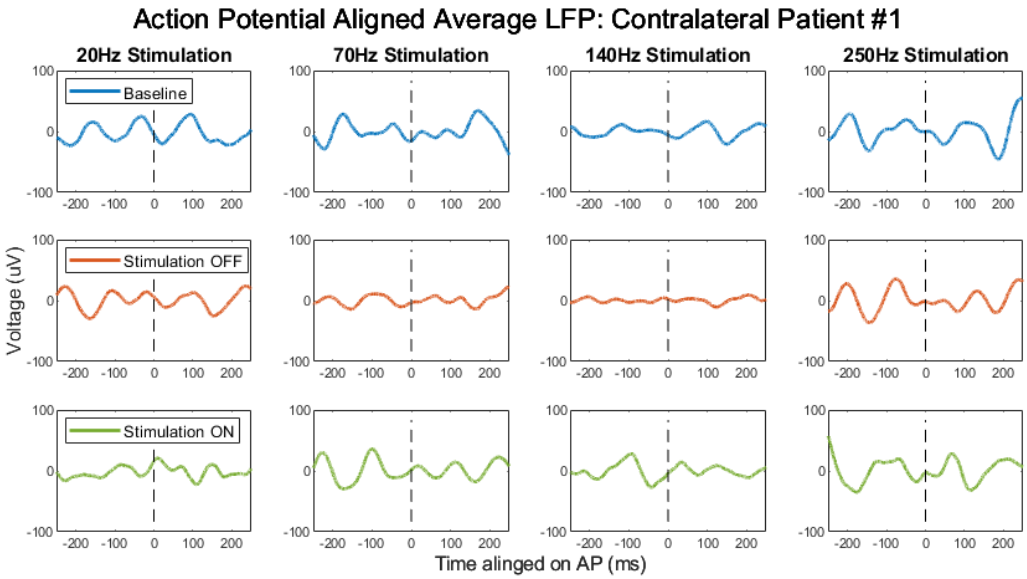

Figure (A3): Plot of action potential aligned average LFPs for each group. Blue signals indicate baseline recordings, red indicate stimulation OFF, and green indicate stimulation ON. No clear differences between signals can be observed.

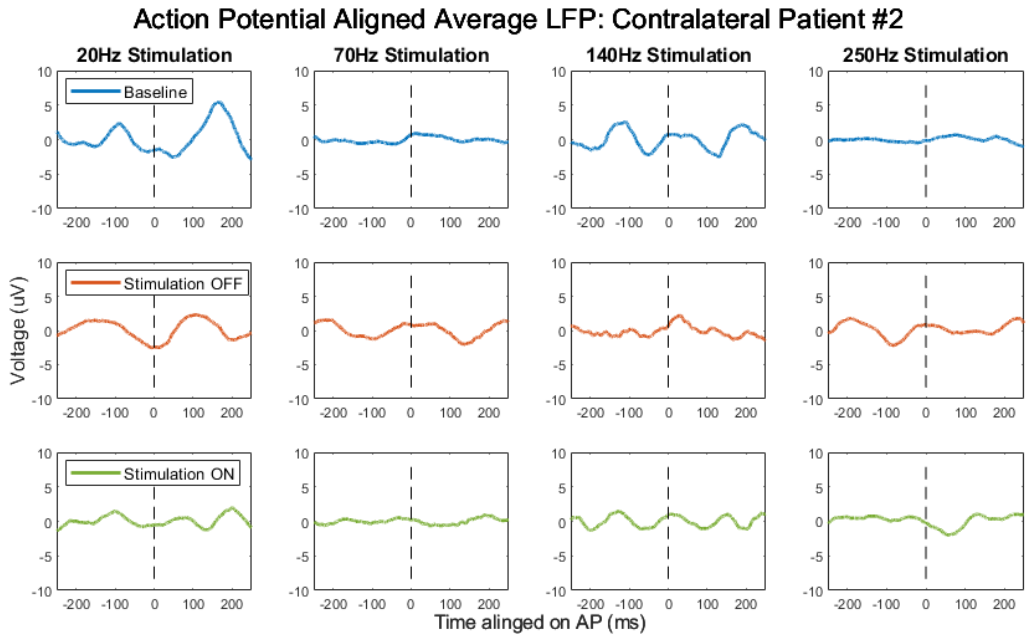

Figure (A4): Plot of action potential aligned average LFPs for each group. Blue signals indicate baseline recordings, red indicate stimulation OFF, and green indicate stimulation ON. No clear differences between signals can be observed.

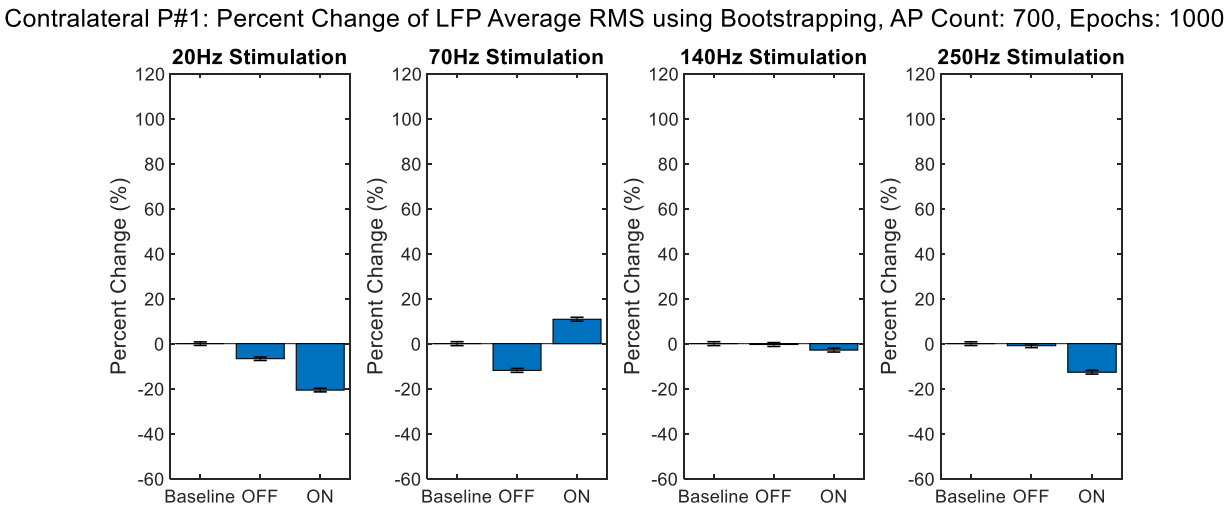

Figure (A5): Contralateral Patient #1. Percent change of APAALFP RMS from baseline. Error bars represent standard error. All values are statistically significant except for groups during stimulation.

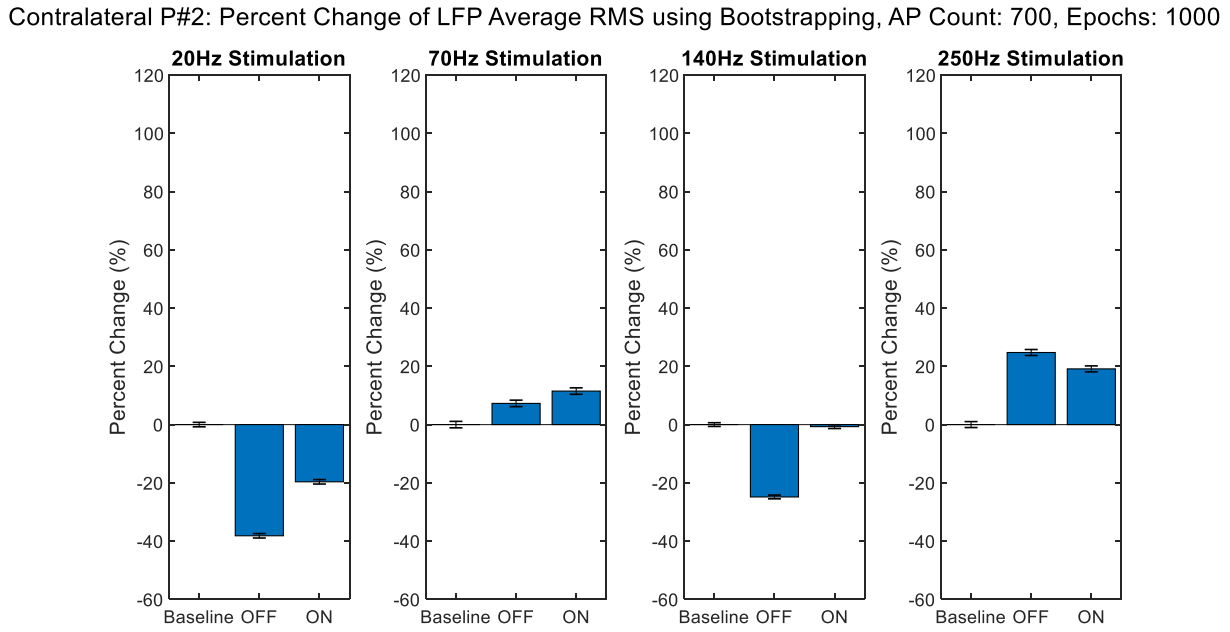

Figure (A6): Contralateral Patient #2. Percent change of APAALFP RMS from baseline. Error bars represent standard error. All values are statistically significant except for Baseline/ON during 140Hz stimulation and OFF/ON during 250Hz stimulation.

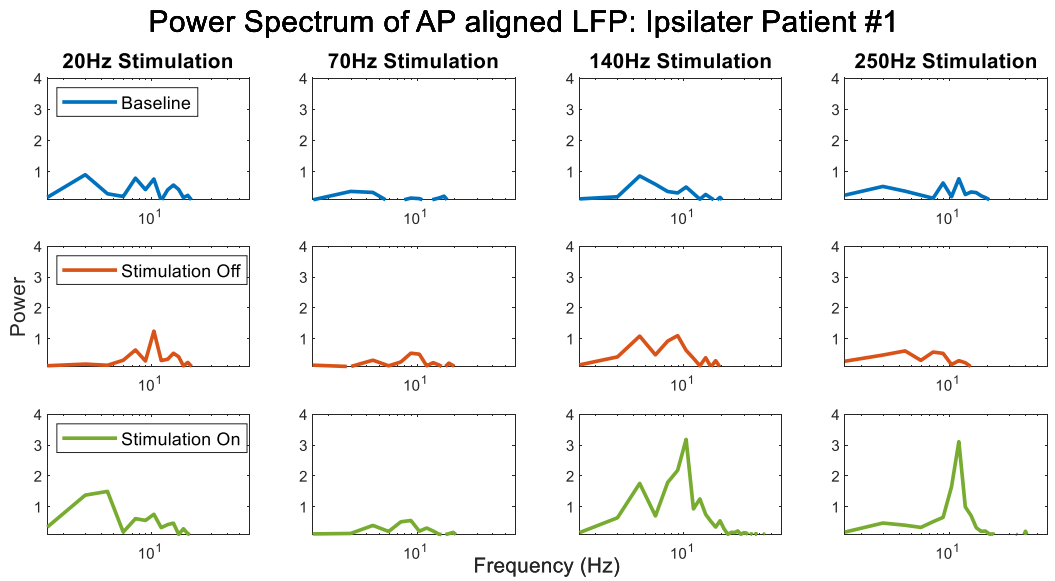

Figure (A7): Power spectrums of all groups for ipsilateral recordings (patient #1). Increase in power at both 4.5Hz & 10.5Hz during 140Hz stimulation. Increase in power at 11Hz during 250Hz stimulation. Increase in power at 2-4Hz during 20Hz stimulation.

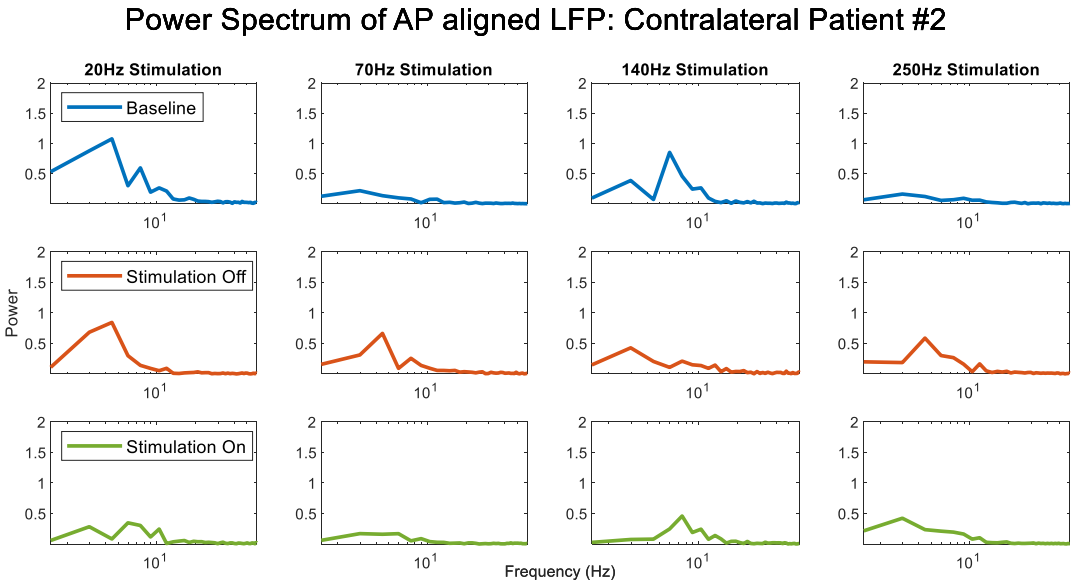

Figure (A8): Power spectrums of all groups for contralateral recording (patient #1). No obvious changes in power spectrum besides possibly an increase in low frequency power during stimulation phase.

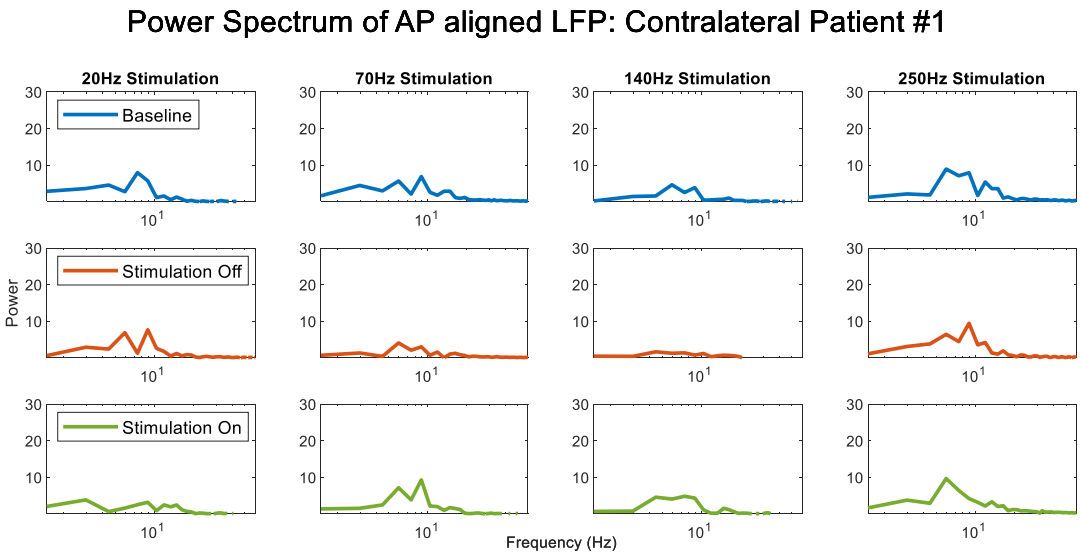

Figure (A9): Power spectrums of all groups for contralateral recording (patient #2). No obvious changes in power spectrum.

Figure (A10): Hardware setup for tremor measurement system. Sparkfun accelerometer attached to wrist. Arduino used to record signal and transmit to TDT system where signal is time synched with neural recording.